Contemporary Engineering Sciences, Vol. 2, 2009, no. 9, 391 - 422

Nonlinear Interactive Multiobjective Optimization Method for Radiotherapy Treatment Planning with Boltzmann Transport Equation

Henri Ruotsalainen

Department of Physics, University of Kuopio
P.O. Box 1627, FI-70211 Kuopio, Finland
Henri.Ruotsalainen@uku.fi

Eeva Boman

Department of Clinical Physiology and Nuclear Medicine
Kuopio University Hospital
P.O. Box 1777, FI-70211 Kuopio, Finland

Kaisa Miettinen

Department of Mathematical Information Technology
P.O. Box 35 (Agora), FI-40014 University of Jyväskylä, Finland

Jouko Tervo

Department of Mathematics and Statistics, University of Kuopio
P.O. Box 1627, FI-70211 Kuopio, Finland

Abstract

In this paper, we present a nonlinear interactive multiobjective optimization method for radiotherapy treatment planning using the Boltzmann transport equation (BTE) in dose calculation. In radiotherapy, the goals are to destroy a tumor with radiation without causing damage to healthy tissue. These goals are conflicting, i.e. when one target is optimized the other will suffer, and the solution is a compromise between them. Our interactive approach is capable of handling multiple and strongly conflicting objectives in a convenient way, and thus the weaknesses of widely used optimization techniques in the field (e.g. defining weights and trial and error planning) can be avoided. In this paper, we use a parameterization technique to make the dose calculation faster

in the BTE model. With our approach, the number of solutions to be calculated is rather small but still informative, planning times can be shortened and plan quality improved by finding only feasible solutions and advantageous trade-offs. Importantly, we used the radiotherapy expert's knowledge to direct the solution process. To demonstrate the advantages, we compare the results with those of the commonly used penalty function method.

Mathematics Subject Classification: 90C29, 90C90

Keywords: Nonlinear multiobjective optimization, Interactive methods, Boltzmann transport equation, Radiotherapy treatment planning optimization

1 Introduction

This year, millions of people all over the world will be diagnosed with cancer. More than half of these patients will be treated with radiation at some point during their lives. Radiation affects the cells' DNA and can kill cancerous cells or prevent them from growing and dividing. Cancerous cells are more susceptible to radiation than healthy ones but radiation affects healthy ones as well. Thus, treatments must be carefully planned so that the effect of radiation is concentrated on cancerous cells while healthy tissue does not receive too much radiation. In this paper, we demonstrate how intelligent multiobjective optimization methods can offer better solutions than the approaches used so far. At the same time, they provide a way to formulate the optimization problem so that the real goals can be considered without missing any information about the solution.

Mathematical models describing the behavior of radiation in a patient (needed for radiotherapy treatment planning) have improved over the years, and the dose distribution can be calculated more accurately. Models based on the Boltzmann transport equation (BTE) have been studied extensively for radiotherapy purposes, and at the moment they are regarded as one of the most promising techniques for dose calculation [32]. Most studies consider the solution of the radiotherapy forward problem, i.e. how to compute the dose within a patient when the treatment settings are given. Recently, there has been interest in using BTE models in solving the radiotherapy inverse problem, i.e. how to solve the treatment settings under some limitations for the dose distribution in the patient [33, 35]. The challenge in using the BTE models is their long computing time. This is why a novel method called parameterization was used in [35] for solving the radiotherapy inverse problem. In this paper, we use the BTE model and the parameterization technique in dose calculation.

There has recently been considerable interest in employing multiobjective optimization in radiotherapy treatment planning (see e.g. [11, 16, 5, 13, 28,

15]). This is because the aim of radiotherapy is to destroy the tumor without affecting the healthy tissue, but, naturally, increasing the dose in the tumor also increases the unwanted dose in the surrounding healthy tissue. Thus, when one target is optimized the other will suffer, and the solution is a compromise between them. This trade-off is complex, and optimization tools capable of handling multiple and conflicting objectives are required. The multiobjective optimization approaches presented in the literature are based on using objective weights defined beforehand, where the objective function is expressed as a weighted sum of objectives (see e.g. [9, 18, 19, 21, 17]). Alternatively, evolutionary algorithms (see e.g. [37, 30]) have been used. These methods have their own difficulties, e.g. it is typically hard to predefine the priorities or weights of the optimization targets (for the weighting method) or they are very time consuming, necessitating a lot of calculation (evolutionary algorithms). Moreover, sometimes information about objectives and even the practical relevance of the objective functions can become blurred if the objectives are expressed as a sum. To avoid all these limitations and to overcome the problems related to BTE modeling in treatment planning optimization, we present an interactive multiobjective optimization approach combined with the parameterized BTE radiotherapy dose calculation model.

In this paper, we apply the nonlinear interactive multiobjective optimization method for BTE model-based radiotherapy treatment planning. Typically, optimization problems in treatment planning are often solved without explicitly emphasizing the multiobjective nature of the problem. In this paper, we exploit the multiobjective nature of the problem in problem formulation and in the interactive solution process, and demonstrate the advantages of our interactive approach. In this approach, the decision maker's (i.e. radiotherapy expert's) knowledge is used during the iterative solution process with the parameterized BTE dose calculation model to direct the search in order to find the most preferred plan, that is, the best Pareto optimal solution, as it is called, between the conflicting criteria. In our earlier research, we have integrated the interactive multiobjective optimization method with a simple pencil beam dose calculation model of intensity modulated radiotherapy [29], and since the results were promising, we now use the deterministic coupled time-independent linear BTE model, which is an integro-partial differential equation, in dose calculation. The BTE model enables more exact and realistic dose calculation. Although the computation of the parameterization is difficult and time-consuming, it has to be done only once before the optimization procedure and thus the BTE model can be used in an interactive multiobjective optimization procedure with consecutive iterations. In addition, since the decision maker directs the solution process interactively, only feasible and interesting Pareto optimal solutions are generated (according to the preferences of the decision maker). Thus, there is no need for lengthy calculations and a large solution

database. With the approach, the desired solution is easily achieved by the decision maker by manipulating the desired values of the objective functions directly. A decision support aid of this kind overcomes the drawbacks of trial and error planning and defining weights beforehand, and planning times can be shortened and plan quality can be improved by finding advantageous trade-offs. The idea of supporting the decision making process and comparing solutions is also presented in [18, 21, 17, 7, 12, 14, 8, 10, 36, 6, 27] but the optimization methods used are not interactive, or those are based on beforehand calculated database of Pareto optimal plans, and the dose is not calculated with the BTE model. In spite of all, it is not well-known how to navigate around in the Pareto set in order to find the final solution.

The rest of the paper is organized as follows. First, a short introduction to the BTE model used in dose calculations is given in Section 2. The model itself is presented in Appendix 1. Thereafter, we discuss the optimization problem in radiotherapy and define the objective functions used in this research (Section 3). In Section 4, after introducing all the information needed about radiotherapy, we discuss multiobjective optimization and present the nonlinear interactive multiobjective optimization method used. Numerical results and discussion of the results are given in Section 5, and finally, conclusions are drawn in Section 6.

2 Dose calculation using a finite element model

Mathematical models describing how radiation behaves have improved continuously, and the dose distribution in a patient can now be calculated quite accurately. Recently, there has been interest in using transport equation models to compute an estimate for the propagation of electrons or photons in tissue instead of the kernel models and Monte Carlo method [33, 35]. The use of the BTE model is becoming more popular as computer power increases, but it is not yet used in clinics because of computational problems. The BTE model takes into account rigorously patient inhomogeneity and scattering effects. Apart from the drawback arising from computation time, the advantages of using a BTE model in radiotherapy dose calculation are clear. Thus, new methods must be developed to enable the use of the BTE model for radiotherapy dose calculations. For this reason, in this paper we use parameterization [35] to shorten the long BTE model dose calculation times in treatment planning optimization. For saving space, the dose calculation model used is presented in Appendix 1.

3 Optimization in radiotherapy

In this section, we specify the goals and objective functions of radiotherapy treatment planning. As mentioned above, the aim of radiotherapy is to destroy the tumor without causing damage to healthy tissue. However, these targets are conflicting since increasing the dose in the tumor also increases the unwanted dose in the surrounding healthy tissue. Thus, the final solution is always a compromise and the trade-off is complex. In the literature, steering the optimization to the solutions most likely to satisfy the radiotherapist has been regarded as a notoriously difficult task, and thus some compromises with the objective function formulation have been made. This is because it is easier to achieve a solution when simplifications are made to the objective functions, but at the same time information about the actual problem will be lost. In this section, we formulate alternative objective functions to satisfy the radiotherapy goals without loss of relevant information while achieving the best possible solution.

3.1 An acceptable solution for radiotherapy treatment planning

We define a patient domain $V \subset \mathbf{R^3}$ containing a target region T (which is a tumor), a critical organ region C (which is a very dose-sensitive healthy organ) and a region of normal tissue N (healthy tissue surrounding T and C). Thus, we have the union $V = \mathrm{T} \cup \mathrm{C} \cup \mathrm{N}$, see Figure 1. Let us assume that we have fields S_l $(l = 1, ..., L)$ from where the radiation flux comes.

We show in the Appendix 1 that the dose $D(x)$ can be obtained from the functional (43), and an acceptable solution for radiotherapy can now be defined. Suppose that D_0 is the prescribed uniform desired dose in tumor T and that D_{C} and D_{N} are the upper bounds of dose in the critical organ C and in normal tissue N, respectively. The limits D_0, D_{C} and D_{N} are defined by a radiotherapy expert according to commonly used dose limits. Note that the tumor, the critical organ and normal tissue may be divided into many separate parts, and dose limits may be different in these parts. Now we can write: determine the incoming flux $u \in L_2(\partial V \times I \times S)$ such that

$$\begin{aligned} D(x) &= D_0, \ x \in \mathrm{T} \\ D(x) &\leq D_{\mathrm{C}}, \ x \in \mathrm{C} \\ D(x) &\leq D_{\mathrm{N}}, \ x \in \mathrm{N} \end{aligned} \tag{1}$$

and that

$$u \geq 0. \tag{2}$$

These requirements are commonly used in clinics and in the literature, to guarantee the acceptability of a treatment plan. In other words, these are the

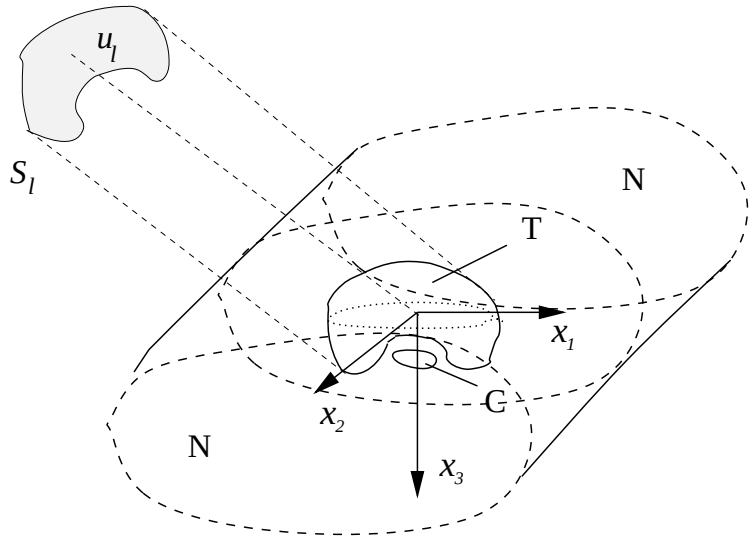

Figure 1: In dose calculation, in field S_l there is flux u_l in the treatment space. The flux comes to the patient domain V which includes regions T, C and N.

minimal requirements the plan must fulfill. Nevertheless, we should point out that the actual goal is to minimize the unwanted dose in total, not only up to the dose limits D_{C} and D_{N}.

Besides the requirements (1), sometimes dose volume constraints can be used (see e.g. [35]). Dose volume constraints may be necessary for critical organs, for example. Radiobiological or biological objective functions can also be included (see e.g. [3, 34, 1]) in some cases, and a bunch of other performance measures can be used in making assessment of the treatment plan. Many of these measures are very important in clinical decision making and they can be used as objective functions in optimization, but we do not use them in this work because of the academic nature of our example.

3.2 Objective functions

Now we describe and formulate the objective functions of the multiobjective optimization problem in such a way that the treatment planning goals and the principles of an acceptable solution (1)-(2) are really taken into account: that is, these objective functions really minimize the harmful radiation in C and N. These objective functions are not often used without constraints, i.e. setting bounds on the dose to the tumor, see e.g. [31]. In addition, with the optimization methods commonly used it is sometimes difficult to steer the solution to the most desired one if the objectives are not formulated as a weighted penalty function penalizing only the dose beyond the defined dose

limits. However, formulating objectives as penalties, in turn, means that the most informative objective functions can not be used and the information about the phenomenon can be lost. To avoid this we define three objective functions according to the wishes of the decision maker (instead of only one) as

$$\tilde{f}_1(\gamma) = ||D_0 - D\gamma||_{L_\infty(\mathrm{T})}, \tag{3}$$

$$\tilde{f}_2(\gamma) = ||D\gamma||_{L_1(\mathrm{C})} \tag{4}$$

and

$$\tilde{f}_3(\gamma) = ||D\gamma||_{L_1(\mathrm{N})}. \tag{5}$$

For computational needs, functions must be discretized. In a discrete form, these functions are (f_2 and f_3 are scaled)

$$f_1(\gamma) = \max_{x \in I_\mathrm{T}}(|D_0 - D\gamma(x)|), \tag{6}$$

$$f_2(\gamma) = \frac{1}{|I_\mathrm{C}|} \sum_{x \in I_\mathrm{C}} |D\gamma(x)| \tag{7}$$

and

$$f_3(\gamma) = \frac{1}{|I_\mathrm{N}|} \sum_{x \in I_\mathrm{N}} |D\gamma(x)|, \tag{8}$$

where I_T, I_C and I_N are selected finite sets of nodes in T, C and N, respectively. $|I_\mathrm{C}|$ and $|I_\mathrm{N}|$ are the numbers of elements of I_C and I_N, respectively.

Here, the objective function f_1 means the maximum dose deviation from a desired dose D_0 in T, and we want to minimize it. The objective functions f_2 and f_3 are the averaged doses in C and N, respectively, which are also to be minimized. The constraint $u \approx S_2\gamma \geq 0$ is also included. These three objective functions really minimize the unwanted (integrated) dose in C and N, not only minimize the dose beyond limits D_C and D_N. We can say that they realize the actual goals of optimization in radiotherapy treatment planning. The use of such objective functions is recommended because radiotherapy experts have observed that the integral dose can be surprisingly high when the critical organs and normal tissue are only kept under a predefined dose limit.

In this paper, a comparison between different optimization approaches is made to demonstrate the convenience of our interactive approach. In the comparison, we use the objective functions presented in [35, 2], where the penalty function method (also called the weighting method in some cases) was used without explicitly emphasizing the multiobjective nature of the problem.

In this case, we can formulate the problem as if we had three objective functions to be minimized as

$$\tilde{f}_4(\gamma) = ||D_0 - D\gamma||^2_{L_2(\mathrm{T})}, \tag{9}$$

$$\tilde{f}_5(\gamma) = ||(D_{\mathrm{C}} - D\gamma)_-||^2_{L_2(\mathrm{C})} \tag{10}$$

and

$$\tilde{f}_6(\gamma) = ||(D_{\mathrm{N}} - D\gamma)_-||^2_{L_2(\mathrm{N})}. \tag{11}$$

For computational needs, these functions also must be discretized. In a discrete form, the functions are (as scaled)

$$f_4(\gamma) = \frac{1}{|I_{\mathrm{T}}|} \sum_{x \in I_{\mathrm{T}}} |D_0 - D\gamma(x)|^2, \tag{12}$$

$$f_5(\gamma) = \frac{1}{|I_{\mathrm{C}}|} \sum_{x \in I_{\mathrm{C}}} |(D_{\mathrm{C}} - D\gamma(x))_-|^2 \tag{13}$$

and

$$f_6(\gamma) = \frac{1}{|I_{\mathrm{N}}|} \sum_{x \in I_{\mathrm{N}}} |(D_{\mathrm{N}} - D\gamma(x))_-|^2. \tag{14}$$

The objective function f_4 controls the violation of the requirement $D_0 = D(x)$ ($x \in \mathrm{T}$). The minimization of f_5 and f_6 is actually a part of a penalty function method for handling constraints and it takes care of the requirements $D(x) \leq D_{\mathrm{C}}$ ($x \in \mathrm{C}$) and $D(x) \leq D_{\mathrm{N}}$ ($x \in \mathrm{N}$). Note that in functions f_5 and f_6, the subscript "$_-$" refers to the negative part of the function. That is, the functions f_5 and f_6 will minimize only the dose which oversteps the preset limits, not all the unwanted dose. With these objective functions, the constraint $u \approx S_2\gamma \geq 0$ must be used.

These objective functions are often used with weighting coefficients in studies presented in the literature because the final solution is thus easy to obtain. However, it is notoriously difficult to set the optimization parameters, e.g. objective weights, to steer the solution process in the direction the decision maker wants when the objectives are in a strong conflict as in this case. These functions are used to guarantee that the solution fulfills the minimum requirements of the plan but, at the same time, the harmful dose is not really minimized and information about the solution is lost due to the use of a quadratic form of functions and penalizing only the dose beyond the predefined dose limits.

In [35, 2], no active constraint handling was used for the constraint $u \approx S_2\gamma \geq 0$, which was formulated as one more objective in the penalty function method

$$\tilde{f}_7(\gamma) = ||S_2\gamma_-||^2_{L_2(\partial V \times I \times S)}, \tag{15}$$

which gets a discrete form (as scaled)

$$f_7(\gamma) = \frac{1}{\max_{x \in I_{\partial V \times I \times S}} S_2\gamma(x)} \sum_{x \in I_{\partial V \times I \times S}} ((S_2\gamma)_-)^2(x). \tag{16}$$

Therefore, the method used in [35, 2] is actually a combination of the ϵ-constraint method (see e.g. [22]) and the penalty function method. The method

used in [35, 2] is sometimes called the weighted sum method or weighting method. Note that it is not the same as the multiobjective optimization method known as the weighting method.

4 Multiobjective optimization

4.1 General notation

A multiobjective optimization problem can be defined as follows [22]

$$\begin{array}{ll} \text{minimize} & \{f_1(\gamma), f_2(\gamma), \ldots, f_k(\gamma)\} \\ \text{subject to} & \gamma \in A, \end{array} \tag{17}$$

where γ is a vector of decision variables from the feasible set $A \subset \mathbf{R^n}$ defined by linear, nonlinear and box constraints. We can denote an objective vector by $\mathbf{f}(\gamma) = (\mathbf{f_1}(\gamma), \mathbf{f_2}(\gamma), \ldots, \mathbf{f_k}(\gamma))^{\mathbf{T}}$. Furthermore, we denote the image of the feasible set by $\mathbf{f}(\mathbf{A}) = \mathrm{Z}$ and call it a feasible objective set.

In multiobjective optimization, optimality is understood in the sense of Pareto optimality [22]. A decision vector $\gamma^{'} \in A$ is Pareto optimal if there does not exist another decision vector $\gamma \in A$ such that $f_i(\gamma) \leq f_i(\gamma^{'})$ for all $i = 1, \ldots, k$ and $f_j(\gamma) < f_j(\gamma^{'})$ for at least one index j. These Pareto optimal solutions form a Pareto optimal set. All the solutions are equally good from a mathematical point of view, and they can be regarded as equally valid compromise solutions of the problem. There exists no trivial mathematical tool in order to find the best solution in the Pareto optimal set because vectors cannot be ordered completely. That is why we need some additional information.

Typically a decision maker who is an expert in the field is needed in order to find the best or most satisfying solution, called the final one, see [22] and references therein. The decision maker can participate in the solution process, and, in one way or another, determine which of the Pareto optimal solutions is the most satisfying to be the final solution. It can be useful for the decision maker to know the ranges of objective function values in the Pareto optimal set. An ideal objective vector $\mathbf{z}^* \in \mathbf{R^k}$ gives lower bounds for the objective functions in the Pareto optimal set and it is obtained by minimizing each objective function individually subject to the constraints. A nadir objective vector $\mathbf{z^{nad}}$ giving upper bounds of objective function values in the Pareto optimal set is usually difficult to calculate, and thus its values are usually only approximated by using pay-off tables, for example (see [22] for details).

The methods developed for multiobjective optimization can be divided into four classes according to the role of the decision maker [22]. There are methods for use when no decision maker is available. In these methods, the final solution is some neutral compromise solution. In the three other classes, the decision maker participates in the solution process beforehand, afterwards or

iteratively: these methods are called the a priori, a posteriori and interactive methods, respectively. It can be difficult for the decision maker to specify preferences before the solution process has started and, on the other hand, generating many Pareto optimal solutions for the decision maker to compare can be computationally costly. It is also problematic to compare many solutions without setting too much cognitive load on the decision maker. Consequently, and encouraged by experiences reported in [29], we concentrate in this paper on interactive methods.

For some reason, interactive methods have not been studied in the field of radiotherapy optimization before. The studies mentioned in the introduction are based on methods with no decision maker, a priori methods, or a posteriori methods. We, however, think that an interactive multiobjective optimization method is ideal for radiotherapy optimization. It makes it possible for the decision maker to control the solution process iteratively and thus learn about the conflicting radiotherapy targets during the optimization. An interactive approach may also involve shorter computing times, because the decision maker directs the solution process and only solutions that he/she is interested in are generated. In this way, trial and error planning can be avoided.

4.2 The interactive multiobjective optimization method

In this paper, we integrate the BTE radiotherapy dose calculation model with an interactive multiobjective optimization method. The method we use is called NIMBUS [24, 22, 26]. This method was selected because it has been successfully used in treatment planning optimization with a simple pencil beam model in [29].

In interactive multiobjective optimization methods, the information given to and required from the decision maker must be easily understandable. The NIMBUS method is based on the idea of classification of objective functions. It is known that classification can be considered an acceptable task for human decision makers from a cognitive point of view [20]. The decision maker participates in the solution process iteratively and continuously in NIMBUS. Finally, he/she decides which of the Pareto optimal solutions obtained is the most desired one. During the solution process, the decision maker classifies objective functions at the current Pareto optimal point into up to five classes. The classes are the following:

- $I^<$ functions whose values should be improved,
- $I^\leq$ functions whose values should be improved up to a desired aspiration level $\hat{z}$,
- $I^=$ functions whose values are satisfactory,

– $I^{\geq}$ functions whose values can be impaired up to a given bound ϵ,

– $I^{>}$ functions whose values can change freely.

Since all the solutions considered are Pareto optimal, the decision maker cannot make a classification where all the objective function values should improve without allowing at least one of the objective functions to be impaired. The aspiration levels and the bounds are elicited from the decision maker during the classification procedure if they are needed.

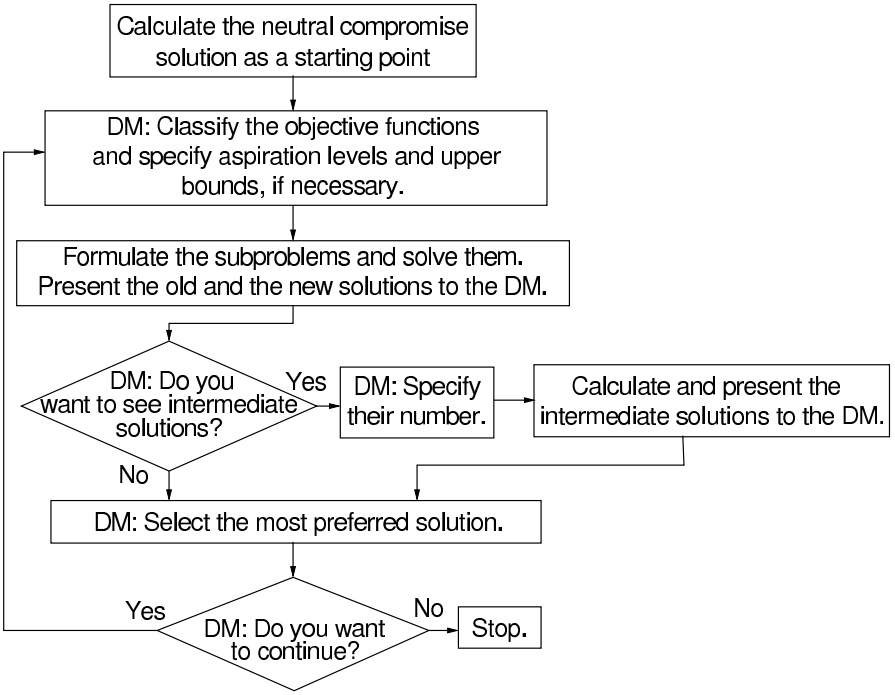

Figure 2: The NIMBUS algorithm.

By classifying the objective functions, the decision maker gives preference information about how the current solution should be improved. Based on that, a scalarized single objective optimization problem (a subproblem, as we call it) can be formed. Here we use a synchronous NIMBUS method [26]. In this method, there are four different subproblems available, so the decision maker can choose weather to see one to four new solutions after each classification. Each subproblem generates a new Pareto optimal solution that satisfies the preferences given in the classification as well as possible, but the preferences are taken into account in slightly different ways [25]. The decision maker can use any solution obtained so far as a starting point for a new classification, and interesting solutions can also be saved in a database, so that the solution process can be continued later from any of them. Alternatively, the decision

maker can generate a desired number of Pareto optimal intermediate solutions between any two Pareto optimal solutions. This capacity differs from many other approaches where intermediate solutions are only approximated (see, e.g. [27]). The subproblems formed are solved with appropriate single objective optimizers. The NIMBUS algorithm is presented in Figure 2. For more information about the NIMBUS algorithm, the scalarizations used and ways of aiding comparison of Pareto optimal solutions generated with different visualizations, see [26].

5 Results

In this section, we solve the radiotherapy optimization problem with the interactive multiobjective optimization method in the first example. In the second example, we solve with our approach another problem which is solved with the penalty function method in [2] and compare the results.

5.1 Test settings

The presented radiotherapy dose calculation model was solved using FEM and only one BTE was used to describe the traveling of artificial particles in a 2D plane ($\mathbf{x} = (\mathbf{x_2}, \mathbf{x_3})$). The photon scattering data was used, but the dose computation was done from the photon flux using artificial stopping powers $\kappa(\mathbf{x}, \mathbf{E})$. The particles were assumed to scatter in the spatial 2D plane. Thus, the angular variable was $\theta \in [0, 2\pi[$ and $\theta = 0$ toward the x_3-axis. This caused an insignificant inaccuracy in the computations of the forward problem because the out of plane scattering was neglected.

The FEM simulations using the SVD parameterization was done in a [-5,5] $\times$ [0,10] cm^2 domain, which consisted of water. The domain was divided into 121 rectangular elements with 144 node points (N_s=144). The elements, node points, and the source nodes for the fields are shown in Figure 3. The angular domain $\theta \in [0, 2\pi[$ was divided into 8 evenly distributed intervals, and the energy domain $E \in [0.1, 10]$ MeV was divided into 3 evenly distributed intervals with 4 node points. Thus, $N_o = 8$, $N_e = 4$ and $N = N_s N_o N_e = 4608$. In the simulations, only inward directions and maximum energy E=10 MeV were allowed in the source nodes, thus $M_e = 1$ and $M_o = 3$. The number of source nodes was $M_s = 32$, and $M = M_s M_o M_e = 96$: hence we had 96 continuous decision variables in this case. The computation of matrix $\mathbf{S}$ (Equation (38)) took about 3 hours, but when the geometry stays unchanged and the source nodes are the same, there is no need to re-calculate the matrix $\mathbf{S}$ between optimization runs. The different regions of the domain T (dark gray), C (light gray), and N (white area) are also shown in Figure 3. The regions T and C are rectangular because we want to prove the efficiency of our

method in handling challenging geometries (non-smooth shapes). In addition, the interactive multiobjective optimization of radiotherapy treatment planning is at its best when T and C are close together, and when targets are strongly conflicting (in clinical head-and-neck and prostate cases, for example).

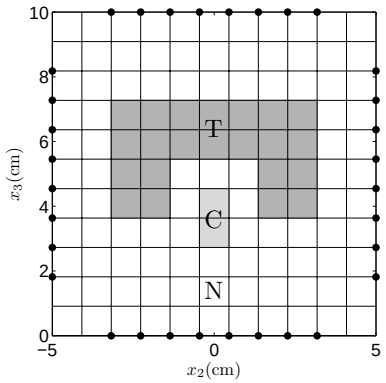

Figure 3: Elements, node points, and source nodes.

All the simulations were carried out with the mathematical software Matlab®. The optimization was made with a personal computer (Pentium® 4 CPU 3.00 GHz with 2 GB central memory). Solving the BTE model, the parameterization and the penalty function method optimization were carried out using a personal computer (Pentium® 4 CPU 2.00 GHz with 2 GB central memory). For multiobjective optimization, an implementation of the NIMBUS method, called IND-NIMBUS® [23], with a local optimizer based on the proximal bundle method [26], was used. In the optimization with the penalty function method, global optimization was done using a simulated annealing algorithm [4] with Matlab®.

5.2 Example 1

In this example, we show how our interactive approach is capable of handling objective functions which are strongly conflicting. Thus, the multiobjective optimization problem is of the form

$$\begin{array}{ll} \text{minimize} & f_1(\gamma), \mathbf{f_2}(\gamma), \mathbf{f_3}(\gamma) \\ \text{subject to} & u \geq 0, \end{array} \tag{18}$$

where γ is a vector of continuous decision variables. In equation (6), the dose limit D_0 was set to 10 Gy, and in this example all the object function values describe dose deviation from desired dose (f_1) or actual dose (f_2 and f_3)

in grays (Gy). The isodose maps (contour plots) presented are plotted from percentual dose values in which D_0 was scaled to 100%.

Initial solution The interactive multiobjective optimization solution process was guided by preference information obtained from a radiotherapy expert, who was acting as a decision maker. The aim of the planning is to ensure the pre-specified dose D_0 and dose distribution in T and to minimize the unwanted dose in C and N. At the beginning, the decision maker was given the initial solution, in which the objective functions had the initial values $f_1 = 5.399$, $f_2 = 3.085$ and $f_3 = 3.274$. The initial solution $\mathbf{f}(\gamma^{\mathbf{1}})$ was produced with typical values of the decision variables and was projected on the Pareto optimal set by IND-NIMBUS®. Figure 4 shows the contours describing the dose distribution in the phantom area and a dose volume histogram calculated from the initial solution values.

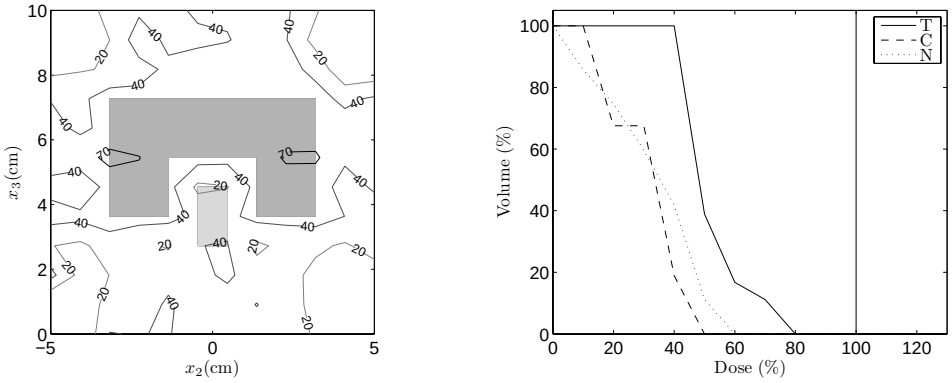

Figure 4: Initial solution. Dose distribution with isodoses 20, 40, 70, 90, 100, where 100% is $D_0 = 10$ Gy, and corresponding dose volume histogram.

In brief, throughout the optimization process, the decision maker had the following aims. He wanted to obtain a solution in which the dose deviation from D_0 in T was minimized. He considered it important that the maximum 10% dose deviation from D_0 should not be overstepped, while the dose in both areas C and N should be as low as possible. As can be seen from the initial objective function values (deviation should be under 10% of D_0, that is, 1 Gy) and from Figure 4, the f_1 value was certainly too high. In the initial solution, the objective functions f_2 and f_3 were nearly at a clinically acceptable level, so the harmful dose in C and N was low but at the same time the deviation from D_0 in T was high. In other words, the dose in the target was too low and the tumor would not be treated properly. Hence, the decision maker wanted to search for a better solution in an iterative way. The decision maker wanted to get four new solution after every classification. All the solutions obtained

during the solution process are collected in Table 1.

1st Classification In the first classification, the decision maker wanted to improve the value of f_1: to decrease the deviation from the desired dose D_0 in T. Simultaneously, he tried to improve f_2 (minimizing the dose in C), but he let f_3 (the dose in N) change freely. This means that he wanted to protect C more efficiently than N. In clinical planning, it is usually more important to save C than N. In brief, the decision maker classified f_1 and f_2 into class $I^<$, and f_3 into class $I^>$ (see classes in Section 4.2).

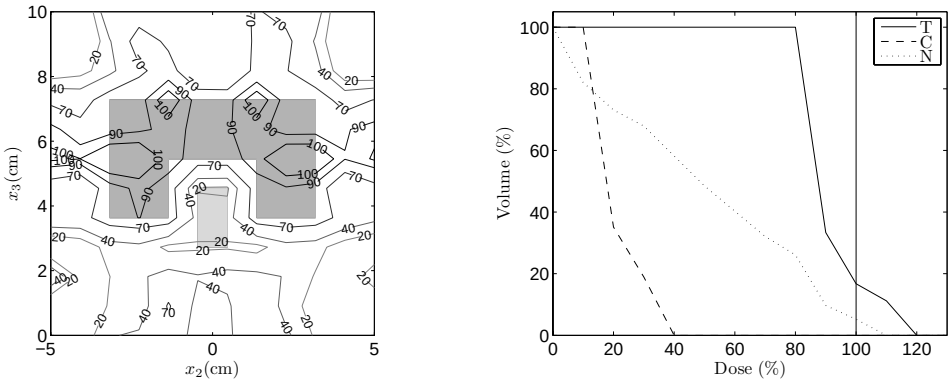

Figure 5: 1st classification. Dose distribution with isodoses 20, 40, 70, 90, 100, where 100% is $D_0 = 10$ Gy, and corresponding dose volume histogram.

After the classification, the decision maker obtained four new solutions. He was able to achieve some improvements and the value of f_1 and f_2 in all the new solutions were at a better level than in the initial solution. At the same time, the objective function f_3 naturally deteriorated. The best of the solutions according to the preferences of the decision maker is shown in Figure 5 ($\mathbf{f}(\gamma^{\mathbf{5}}) = (\mathbf{1.529}, \mathbf{2.170}, \mathbf{4.981})$). As can be seen, the dose in C is low. Nevertheless, the decision maker was not satisfied with the solution because the objective functions f_1 and f_3 were not at acceptable levels; the dose deviation from the desired dose D_0 in T was too high, likewise the harmful dose in N. Since the solution was not clinically desirable, the decision maker wanted to classify the objective functions again, and used the presented solution as a starting point of a new classification.

2nd Classification In the second classification, the decision maker wanted to guarantee a good level of f_1 (class $I^<$), but now he was ready to impair f_2 up to a bound 3 (Gy). Hence, he classified f_2 into class $I^\geq$. Simultaneously he wanted to improve the objective function f_3, that is, he chose classification $I^\leq$ and the desired aspiration level was 3 (Gy).

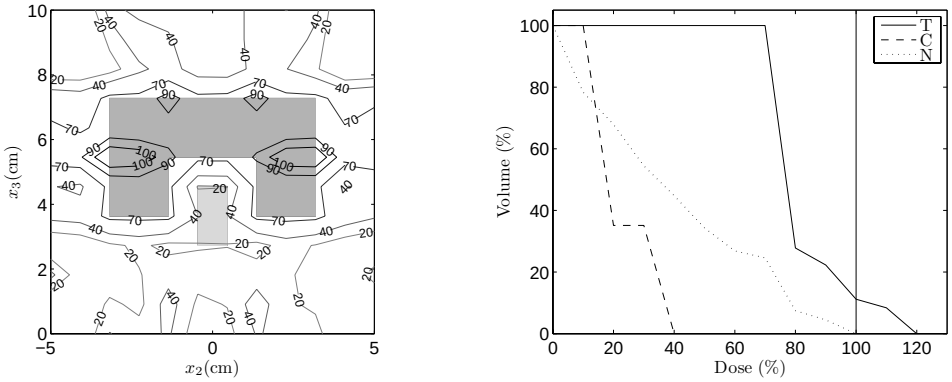

Figure 6: 2nd classification. Dose distribution with isodoses 20, 40, 70, 90, 100, where 100% is $D_0 = 10$ Gy, and corresponding dose volume histogram.

After the second classification, the decision maker obtained four new solutions. He obtained only one solution ($\mathbf{f}(\gamma^{\mathbf{7}}) = (\mathbf{0.765}, \mathbf{2.584}, \mathbf{5.608})$) in which the objective function f_1 (which he considered to be very important) was at a clinically acceptable level, but the other objective function values were worse. In other solutions obtained, f_1 was not good enough, but f_3 was very good. In other words, if the function f_1 was at a good level, the function f_3 was too poor, and vice versa. The decision maker understood that the aspiration level and the upper bound he set were too demanding, and wanted to classify the objective functions again. He used the solution $\mathbf{f}(\gamma^{\mathbf{9}}) = (\mathbf{2.324}, \mathbf{2.525}, \mathbf{3.993})$ (Figure 6) as a starting point of a new classification.

3rd Classification and final solution The decision maker knew that if he wanted to improve the value of f_1, he should let f_2 and f_3 deteriorate. The decision maker felt he was close to the most satisfying solution, which is why he set an aspiration level for f_1 and upper bounds for f_2 and f_3. The objective function f_1 should be better than 0.999 (Gy) and the bound for both f_2 and f_3 was 4 (Gy). That is, he made the classification f_1 to $I^{\leq}$ (aspiration level 0.999 (Gy)), and f_2 and f_3 to $I^{\geq}$ (bound 4 (Gy)).

Again, the decision maker asked for and obtained four new solutions. One of them ($\mathbf{f}(\gamma^{\mathbf{13}}) = (\mathbf{0.985}, \mathbf{2.475}, \mathbf{4.518})$) was an absolutely satisfying compromise and the decision maker felt he was able to make the final decision. He was looking for a solution with as uniform a dose in T as possible and where the preferences concerning dose limitations were satisfied. He achieved a solution in which the deviation from the desired dose D_0 in T was satisfactory (f_1=0.985, which is under 10% of D_0), and simultaneously the unwanted dose in C (f_2=2.475) and in N (f_3=4.518) was as small as could reasonably be achieved. This can also be seen in Figure 7. This solution $\mathbf{f}(\gamma^{\mathbf{13}})$ was the most

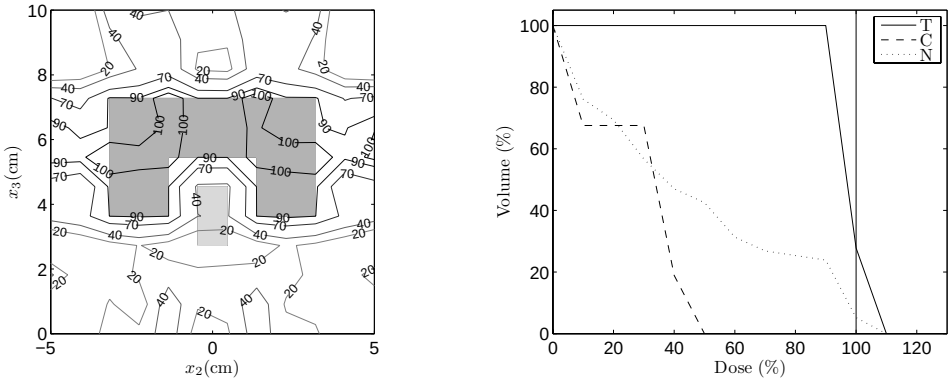

Figure 7: Optimal dose distributions with isodoses 20, 40, 70, 90, 100, where 100% is $D_0 = 10$ Gy, and corresponding dose volume histograms.

Table 1: Example 1: Summary of interactive solution process. Aspiration levels and bounds used are denoted as superscripts in the classification notation.

Solution	f_1(Gy)	f_2(Gy)	f_3(Gy)
Ideal	0.274	0.001	0.008
Nadir	10.398	7.349	6.475
Initial solution			
$\mathbf{f}(\gamma^{\mathbf{1}})$	**5.399**	**3.085**	**3.274**
1st classification	$I^{<}$	$I^{<}$	$I^{>}$
$\mathbf{f}(\gamma^{\mathbf{2}})$	2.990	1.847	4.668
$\mathbf{f}(\gamma^{\mathbf{3}})$	3.060	2.013	4.621
$\mathbf{f}(\gamma^{\mathbf{4}})$	1.533	1.182	5.150
$\mathbf{f}(\gamma^{\mathbf{5}})$	**1.529**	**2.170**	**4.981**
2nd classification	$I^{<}$	$I^{\geq 3}$	$I^{\leq 3}$
$\mathbf{f}(\gamma^{\mathbf{6}})$	2.463	2.462	4.329
$\mathbf{f}(\gamma^{\mathbf{7}})$	0.765	2.584	5.608
$\mathbf{f}(\gamma^{\mathbf{8}})$	3.061	2.092	3.923
$\mathbf{f}(\gamma^{\mathbf{9}})$	**2.324**	**2.525**	**3.993**
3rd classification	$I^{\leq 0.999}$	$I^{\geq 4}$	$I^{\geq 4}$
$\mathbf{f}(\gamma^{\mathbf{10}})$	1.483	4.223	4.309
$\mathbf{f}(\gamma^{\mathbf{11}})$	1.078	4.285	4.483
$\mathbf{f}(\gamma^{\mathbf{12}})$	1.548	4.071	4.148
$\mathbf{f}(\gamma^{\mathbf{13}})$	**0.985**	**2.475**	**4.518**

preferred one to be the final solution according to the decision maker's exper-

tize in radiotherapy. A summary of the solution process and trade-offs are presented in Table 1, including the steps taken by the decision maker and the solutions selected at each iteration (denoted in bold face). Table 1 also shows information about the approximate objective function ranges in the Pareto optimal set as discussed in Section 4.1. Information of this kind can be easily obtained with the approach used and this enables the decision maker to learn and to analyze the interrelationships between the objectives and compare solutions.

Discussion In this example, we show how our interactive approach can handle the strongly conflicting objective functions in a radiotherapy case. Generally in the literature, it is said that strongly conflicting objective functions are notoriously difficult to steer to the solutions most likely to satisfy the decision maker (a radiotherapist). This is because the objective function have typically been expressed as a sum where practical information about the functions could be lost, or it may be hard to define objective weights beforehand because they are not so intuitive. In our approach, practical information about every objective function was maintained, e.g. the objective function values described averaged doses, not uninformative quadratic sums of doses. As can be seen in this example, the objective functions really illustrated how the dose behaved. The function f_1 described a maximum dose deviation from a desired dose and the goodness of the objective function value was easy to understand. In addition, the functions f_2 and f_3 were the averaged doses in C and N, respectively. In this way, the dose could really be minimized in C and N. As can be seen in Table 1, with our approach with the objective functions $f_1 \dots f_3$, the most satisfying solution was not hard to find by manipulating desired values of objective functions directly (not the weights). Thus, only a few iterations and calculations of Pareto optimal solutions were needed.

In treatment planning, the interactive multiobjective optimization approach made it possible for the decision maker to learn about the conflicting dose distribution targets and their interrelationships. Moreover, the thorough decision maker can see what happens when he/she directs the solution process in different ways. Good and unique solutions, which are hard to obtain without a decision support aid of this kind, can be found to satisfy the therapy plan.

Note also that computing times were short: only about one to two minutes per classification (with a PC). The most time-consuming part was solving the BTE forward problem. In the parameterization procedure, the matrix $\mathbf{S}$ is calculated with SVD, which took approximately three hours. Since the matrix $\mathbf{S}$ is solved only once there is no need to re-solve it if the geometry stays unchanged. Once the matrix $\mathbf{S}$ has been found, the optimization method is not a bottleneck for more complicated simulation models.

5.3 Example 2

For comparison, an optimization problem presented in [2] was solved with our multiobjective optimization approach, and here we compare the results with those of the presented in [2]. In [2], the penalty function method was used without emphasizing the problem's multiobjective nature, and the optimization problem was

$$\text{minimize} \quad f_{wm} = \sum_{i=4}^{7} c_i f_i(\gamma), \tag{19}$$

where c_i $(i = 4, ..., 7)$ were positive weights set as $c_4 = 3$, $c_5 = 1.5$, $c_6 = 0.5$, $c_7 = 100$, and the threshold values used in (12)-(14) were $D_0 = 10$ (Gy) (in T), $D_N = 5$ (Gy) (in N) and $D_C = 2$ (Gy) (in C). A global single objective solver had to be used to solve the weighted problem (19) and this took about 20 minutes [2].

The aim of the planning was to ensure the pre-specified dose D_0 and dose distribution in T. In addition, in C and N, the dose was penalized if the threshold values 20% (2 Gy) and 50% (5 Gy) of the D_0, respectively, were overstepped.

On the other hand, the decision maker solved the problem

$$\begin{array}{ll} \text{minimize} & \{f_4(\gamma), \mathbf{f_5}(\gamma), \mathbf{f_6}(\gamma)\} \\ \text{subject to} & u \geq 0 \end{array} \tag{20}$$

with our approach in an iterative and interactive way, as in Example 1. During the solution process, the decision maker used three classifications until he obtained a satisfactory solution. All the solutions generated are shown in Table 2, and the solutions used as a starting point for a new classification are denoted in bold face. Note that the objective function values are quadratic sums of dose differences, thus the physical meaning of the value gets blurred if the unit used is still gray (Gy). The final solution is presented in Figure 8, on the left. As can be seen in Figure 8, the predefined dose limit in T is overstepped, and the entire T did not get the 90% of D_0 dose. Nevertheless, this solution $\mathbf{f}(\gamma^{\mathbf{9}}) = (\mathbf{0.985}, \mathbf{0.512}, \mathbf{6.028})$ was the most preferred one to be the final solution according to the decision maker's radiotherapy expertize because he was satisfied with the dose in C and N. For comparison, the final solution obtained with the penalty function method in [2] is presented in Figure 8, on the right.

Discussion In this example, the results of our interactive approach and the those of the penalty function method can be compared (Figure 8 and Table 3). We can see that the final treatment plans are of the same kind but the advantages of our approach are clear when the efficiency of the optimization process is considered. As can be seen from the results, with our approach we could see

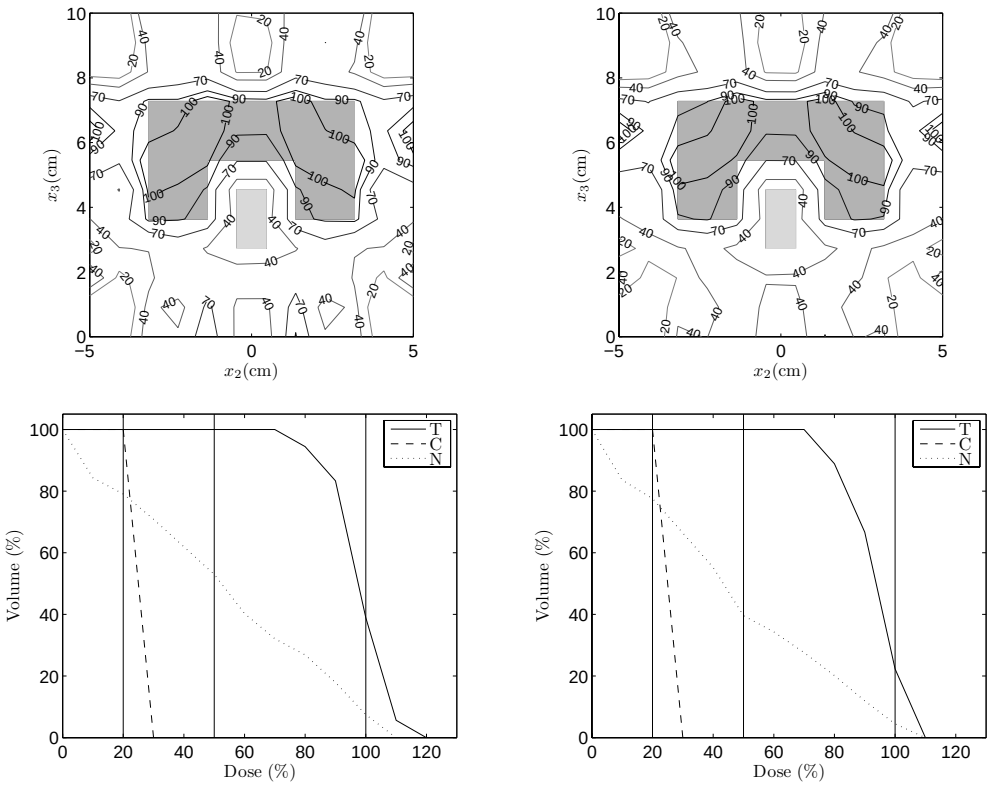

Figure 8: On the left, the solution using our approach and, on the right, the solution using the penalty function method [2]. Optimal dose distributions with isodoses 20, 40, 70, 90, 100, where 100% is $D_0 = 10$ Gy, and corresponding dose volume histograms where the predefined dose limits (vertical lines) are plotted.

in an understandable manner how the solution process progressed and how the new radiotherapy treatment plan fulfilled the decision maker's requirements after every iteration concerning the requirements of the radiotherapy process. In this way, we could avoid the time-consuming trial and error planning and re-optimization which happens in the penalty function method if the plan is not satisfactory or the weighting coefficients are not optimally chosen. For example, we can see in Figure 8, in the solution obtained with the penalty function method, that all the corners of T are outside the 90% isodose, which is not desirable at all. For comparison, with interactive multiobjective optimization, only the corners of T nearest to C were outside the 90% isodose. It seems that the solution of the penalty function method was not the most satisfying for the decision maker, and new weighting coefficients should be discovered, and the time-consuming optimization procedure has to be repeated if the decision

Table 2: Example 2: Summary of interactive solution process. Bound used is denoted as superscripts in the classification notation.

Solution	f_4(Gy)	f_5(Gy)	f_6(Gy)
Ideal	0.001	0	0
Nadir	75.156	32.559	19.175
Initial solution			
$\mathbf{f}(\gamma^{\mathbf{1}})$	**7.188**	**3.121**	**1.014**
1st classification	$I^<$	$I^>$	$I^>$
$\mathbf{f}(\gamma^{\mathbf{2}})$	0.067	22.568	7.505
$\mathbf{f}(\gamma^{\mathbf{3}})$	0.001	31.831	8.825
$\mathbf{f}(\gamma^{\mathbf{4}})$	**0.090**	**21.299**	**7.336**
2nd classification	$I^<$	$I^<$	$I^>$
$\mathbf{f}(\gamma^{\mathbf{5}})$	**1.173**	**5.000**	**3.395**
$\mathbf{f}(\gamma^{\mathbf{6}})$	1.363	5.590	3.346
$\mathbf{f}(\gamma^{\mathbf{7}})$	0.004	19.569	9.853
$\mathbf{f}(\gamma^{\mathbf{8}})$	1.429	5.523	3.309
3rd classification	$I^<$	$I^<$	$I^{\geq 7}$
$\mathbf{f}(\gamma^{\mathbf{9}})$	**0.985**	**0.512**	**6.028**
$\mathbf{f}(\gamma^{\mathbf{10}})$	0.098*	9.764	7.595
$\mathbf{f}(\gamma^{\mathbf{11}})$	0.001	25.795	9.009
$\mathbf{f}(\gamma^{\mathbf{12}})$	0.098*	9.760	7.594

* Pareto optimality is hidden due to the rounding

maker wants to improve the solution. On the other hand, in interactive multiobjective optimization, since the decision maker directed the solution process only interesting Pareto optimal solutions needed to be generated.

Table 3: Interactive multiobjective optimization vs. penalty function method.

	Interactive MOO	Penalty function method
f_4(Gy)	0.985	1.287
f_5(Gy)	0.512	0.368
f_6(Gy)	6.028	4.834
Neg. flux	0	0.001

Furthermore, we noticed that the physical feasibility of the solutions obtained is an issue. With the penalty function method, the constraint $u \geq 0$ was included in the objective function: that is, there should be no radiation coming

outward from the phantom, because only radiation flux inward is physically feasible. Nevertheless, in the solution obtained, there was negative flux (0.001 units), as can be seen in Table 3, and this affects the solution significantly. It eliminates dose in the edges of the phantom, and this affects the value of the sixth objective function. Consequently, the solution of the penalty function method was not physically feasible. In Table 3, since objective function f_6 describes the dose in N, the solution obtained with the penalty function method (or the value describing the dose in N) is unrealistically good. However, this is likely to remain unnoticed.

In our multiobjective optimization approach, $u \geq 0$ could be treated as a constraint, which meant that there was no negative flux in the solution. Thus, besides the solution being somewhat better in handling the dose in the target, the solution obtained with our approach was automatically physically feasible, unlike the other one. Without interactive multiobjective optimization, the infeasibility of the solution would not be noticed because, in the penalty function method the objectives are expressed as a sum that hides the negative flux value.

When comparing the dose volume histogram obtained in Example 1 with that obtained in Example 2, we see that with the functions $f_1 \dots f_3$, T obtained a steeper curve to the zero than with the objective functions $f_4 \dots f_6$. In addition, a similar trend can be seen at the beginning of the C and N curve. This is due to the better choice of objective functions: harmful doses in C and N are really minimized, not only penalizing beyond the predefined dose limits (2 Gy and 5 Gy, respectively). Thus, we can say that formulating the problem as a genuine multiobjective optimization problem and solving it with an interactive method has many advantages. Besides the ones discussed so far, it is important to point out that our new formulation produced a convex problem that could be solved with a computationally efficient local optimization method, whereas the old formulation necessitated using a computationally costly global optimization method. In addition, although we obtained somewhat better results with interactive multiobjective optimization than with the penalty function method in Example 2 (with objective functions $f_4 \dots f_6$), our approach is at its best in challenging situations such as Example 1 where the objective functions are formulated to describe better the radiotherapy optimization targets.

6 Conclusion

New treatment machines provide an opportunity to treat cancer patients in more effective ways but, at the same time, they make the radiotherapy modeling and optimization in treatment planning more demanding. The aim of this paper was not only to obtain an optimal radiotherapy treatment plan,

but also to reveal the advantages of interactive multiobjective optimization in radiotherapy treatment planning and to encourage further research in this direction.

In this paper, we present an interactive multiobjective optimization approach combined with the novel parameterized BTE radiotherapy dose calculation model. This was done because we wanted to avoid the limitations of the optimization techniques widely used, and because the advantages of using the BTE model in dose calculations are obvious. Via parameterization, the BTE dose calculation model is so fast that it can be used in interactive multiobjective optimization.

In our approach, the decision maker's knowledge is used during the iterative solution process to direct the optimization in order to find the most preferred plan, that is, the best Pareto optimal solution, between the conflicting radiotherapy targets. A decision support aid of this kind overcomes the drawbacks of trial and error planning, and planning times can be shortened and plan quality improved by finding advantageous trade-offs and finding only feasible solutions by manipulating the desired values of the objective functions directly (not the weights). Our interactive approach is capable of handling radiotherapy objectives which are strongly conflicting. Thus, we were able to describe the objective functions in a way that really minimized the unwanted dose.

Our BTE model is 3D spatially. Nevertheless, we were able to use it in two-dimensional planning only because of the long computing time of matrix **S**. Although the research documented in this paper is academic, the results are promising. In the future, the computational problems can be overcome, and the approach is worth further study in clinical and 3D cases.

ACKNOWLEDGEMENTS. This work was financially supported by Tekes, the Finnish Funding Agency for Technology and Innovation, and also partly by the Jenny and Antti Wihuri Foundation. Thanks to Mr. Vesa Ojalehto, M.Sc., and Ms. Elina Madetoja, Ph.D., for technical support. Special thanks to Prof. Jari Hämäläinen for enabling the study.

References

[1] M. Alber and R. Reemtsen. Intensity modulated radiotherapy treatment planning by use of a barrier-penalty multiplier method. *Optimization Methods and Software*, 22:391–411, 2007.

[2] E. Boman. *Radiotherapy Forward and Inverse Problem Applying Boltzmann Transport Equation.* University of Kuopio, Department of Physics, Kuopio, Finland, 2007. Doctoral thesis.

[3] A. Brahme. Treatment optimization using physical and radiobiological objective functions. In A. E. Smith, editor, *Radiation Therapy Physics*, pages 209–245. Springer, 1995.

[4] A. Corana, M. Marchesi, C. Martini, and S. Ridella. Minimizing multimodal functions of continuous variables with the "simulated annealing" algorithm. *ACM Transactions on Mathematical Software*, 13:262–280, 1987.

[5] C. Cotrutz, M. Lahanas, C. Kappas, and D. Baltas. A multiobjective gradient-based dose optimization algorithm for external beam conformal radiotherapy. *Physics in Medicine and Biology*, 46:2161–2175, 2001.

[6] D. Craft and T. Bortfeld. How many plans are needed in an IMRT multiobjective plan database? *Physics in Medicine and Biology*, 53:2785–2796, 2008.

[7] D. Craft, T. Halabi, and T. Bortfeld. Exploration of tradeoffs in intensity-modulated radiotherapy. *Physics in Medicine and Biology*, 50:5857–5868, 2005.

[8] D. Craft, T. Halabi, H. A. Shih, and T. Bortfeld. An approach for practical multiobjective IMRT treatment planning. *International journal of radiation oncology*Biology*Physics*, 69:1600–1607, 2007.

[9] M. Ehrgott and R. Johnston. Optimization of beam directions in intensity modulated radiation therapy planning. *OR Spectrum*, 25:251–264, 2003.

[10] M. Ehrgott and I. Winz. Interactive decision support in radiotherapy treatment planning. *OR Spectrum*, 30:311–329, 2008.

[11] O. C. L. Haas, K. J. Burnham, and J. A. Mills. Optimization of beam orientation in radiotherapy using planar geometry. *Physics in Medicine and Biology*, 43:2179–2193, 1998.

[12] T. Halabi, D. Craft, and T. Bortfeld. Dose-volume objectives in multicriteria optimization. *Physics in Medicine and Biology*, 51:3809–3818, 2006.

[13] H. W. Hamacher and K.-H. Küfer. Inverse radiation therapy planning - a multiple objective optimization approach. *Discrete Applied Mathematics*, 118:145–161, 2002.

[14] A. L. Hoffmann, A. Y. D. Siem, D. den Hertog, J. H. A. M. Kaanders, and H. Huizenga. Derivate-free generation and interpolation of convex Pareto optimal IMRT plans. *Physics in Medicine and Biology*, 51:6349–6369, 2006.

[15] A. Holder. Partitioning multiple objective optimal solutions with applications in radiotherapy design. *Optimization and engineering*, 7:501–526, 2006.

[16] K.-H. Küfer, H. W. Hamacher, and T. R. Bortfeld. A multicriteria optimization approach for inverse radiotherapy planning. In T. R. Bortfeld and W. Schlegel, editors, *Proceedings of the XIIIth ICCR*, pages 26–29. Springer, Berlin, 2000.

[17] K.-H. Küfer, M. Monz, A. Scherrer, P. Süss, F. Alonso, A. S. A. Sultan, Th. Bortfeld, D. Craft, and Chr. Thieke. Multicriteria optimization in intensity modulated radiotherapy planning. In *Berichte des Fraunhofer ITWM*. 2005. 77.

[18] K.-H. Küfer, A. Scherrer, M. Monz, F. Alonso, H. Trinkaus, T. Bortfeld, and C. Thieke. Intensity-modulated radiotherapy - a large scale multicriteria programming problem. *OR Spectrum*, 25:223–249, 2003.

[19] M. Lahanas, E. Schreibmann, and D. Baltas. Multiobjective inverse planning for intensity modulated radiotherapy with constraint-free gradient-based optimization algorithms. *Physics in Medicine and Biology*, 48:2843–2871, 2003.

[20] O. Larichev. Cognitive validity in design of decision aiding techniques. *Journal of Multicriteria Decision Analysis*, 1:127–138, 1992.

[21] J. Meyer, M. H. Phillips, P. S. Cho, I. Kalet, and J. N. Doctor. Application of influence diagrams to prostate intensity-modulated radiation therapy plan selection. *Physics in Medicine and Biology*, 49:1637–1653, 2004.

[22] K. Miettinen. *Nonlinear Multiobjective Optimization*. Kluwer, Boston, 1999.

[23] K. Miettinen. IND-NIMBUS for demanding interactive multiobjective optimization. In T. Trzaskalik, editor, *Multiple Criteria Decision Making '05*, pages 137–150. The Karol Adamiecki University of Economics, Katowice, 2006.

[24] K. Miettinen and M. M. Mäkelä. Interactive bundle-based method for nondifferentiable multiobjective optimization: NIMBUS. *Optimization*, 34:231–246, 1995.

[25] K. Miettinen and M. M. Mäkelä. On scalarizing functions in multiobjective optimization. *OR Spectrum*, 24:193–213, 2002.

[26] K. Miettinen and M. M. Mäkelä. Synchronous approach in interactive multiobjective optimization. *European Journal of Operational Research*, 170:909–922, 2006.

[27] M. Monz, K. H. Küfer, T. R. Bortfeld, and C. Thieke. Pareto navigation - algorithmic foundation of interactive multi-criteria IMRT planning. *Physics in Medicine and Biology*, 53:985–998, 2008.

[28] H. E. Romeijn, J. F. Dempsey, and J. G. Li. A unifying framework for multi-criteria fluence map optimization models. *Physics in Medicine and Biology*, 49:1991–2013, 2004.

[29] H. Ruotsalainen, E. Boman, K. Miettinen, and J. Hämäläinen. Interactive multiobjective optimization for IMRT. *Working Papers*, W-409, 2006. Available at http://hsepubl.lib.hse.fi/pdf/wp/w409.pdf.

[30] E. Schreibmann, M. Lahanas, L. Xing, and D. Baltas. Multiobjective evolutionary optimization of the number of beams, their orientations and weights for intensity-modulated radiation therapy. *Physics in Medicine and Biology*, 49:747–770, 2004.

[31] D. M. Shepard, M. C. Ferris, G. H. Olivera, and T. R. Mackie. Optimization the delivery of radiation therapy to cancer patients. *SIAM Review*, 41:721–744, 1999.

[32] H Tagziria. Review of monte carlo and deterministic codes in radiation protection and dosimetry. In *NLP Report*. Teddington, 2000.

[33] J. Tervo, P. Kolmonen, M. Vauhkonen, L. M. Heikkinen, and J. P. Kaipio. A finite-element model of electron transport in radiation therapy and a related inverse problem. *Inverse Problems*, 15:1345–1361, 1999.

[34] J. Tervo, T. Lyyra-Laitinen, P. Kolmonen, and E. Boman. An inverse treatment planning model for intensity modulated radiation therapy with dynamic MLC. *Applied Mathematics and Computation*, 135:227–250, 2003.

[35] J. Tervo, M. Vauhkonen, and E. Boman. Optimal control model for radiation therapy inverse planning applying the boltzmann transport equation. *Linear Algebra and Its Applications*, 428:1230–1249, 2008.

[36] C. Thieke, K.-H. Küfer, M. Monz, A. Scherrer, F. Alonso, U. Oelfke, Debus J. Huber, P. E., and T. Bortfeld. A new concept for interactive radiotherapy planning with multicriteria optimization: first clinical evaluation. *Radiotherapy and Oncology*, 85:292–298, 2007.

[37] X. Wu and Y. Zhu. An optimization method for importance factors and beam weights based on genetic algorithms for radiotherapy treatment planning. *Physics in Medicine and Biology*, 46:1085–1099, 2001.

Appendix 1

Dose calculation using a finite element model: the Boltzmann transport equation model

Here, the BTE model is briefly described: for further information, see [35]. Physically, the BTE model is based on particle equilibrium in infinitesimally small voxels of tissue. In the case of radiotherapy, it is appropriate to use the stationary form of the BTE. In this case, taking into account elastic collision, inelastic collision and deceleration radiation, the model consists of a coupled system of stationary linear integro partial differential equations

$$\begin{aligned} \Omega \cdot \nabla \psi_1 + K_1(\psi_1, \psi_2, \psi_3) &= Q_1(x, E, \Omega) \\ \Omega \cdot \nabla \psi_2 + K_2(\psi_1, \psi_2, \psi_3) &= Q_2(x, E, \Omega) \\ \Omega \cdot \nabla \psi_3 + K_3(\psi_1, \psi_2, \psi_3) &= Q_3(x, E, \Omega), \end{aligned} \tag{21}$$

where $\psi_j = \psi_j(x, E, \Omega)$ $(j = 1, 2, 3)$ are the phase space densities for photons, electrons and positrons, respectively. The variable $x = (x_1, x_2, x_3)$ is a point in the patient domain $V \subset \mathbf{R^3}$. Particle energy in denoted by E. The surface of the unit sphere in $\mathbf{R^3}$ is denoted by S, and $\Omega = (\cos\varphi \sin\theta, \sin\varphi \sin\theta, \cos\theta) =: h(\varphi, \theta)$ is a point on S, where φ and θ are standard spherical coordinates on surface S.

The functions $K_j(\psi_1, \psi_2, \psi_3)$ $(j = 1, 2, 3)$ are collision terms combining attenuation and secondary production resulting from the above-mentioned different kinds of interactions, and K_1, K_2, K_3 are linear operators of $\psi := (\psi_1, \psi_2, \psi_3)$. Finally, $Q_j(x, E, \Omega)$ $(j = 1, 2, 3)$ are the source terms, which are typically zero in external radiotherapy, as also in this case. In the following, we denote the system (21) in a compact way by

$$(\Omega \cdot \nabla + K)\psi = Q. \tag{22}$$

Boundary conditions and variational form

We consider the external photon radiation by setting boundary conditions for the photon inflow [35]. We assume that the boundary of the patient domain ∂V is a piecewise smooth Lipschitz boundary. Thus, the outward normal $\nu(x)$ exists and is continuous on ∂V even though there might exits a set with surface measure zero.

A typical photon inflow boundary condition for the solution ψ is of the form

$$\begin{aligned} \psi_2(x, E, \Omega) &= \psi_3(x, E, \Omega) = 0 \text{ for } (x, E, \Omega) \in \partial V \times I \times S \\ &\quad \text{such that } \Omega \cdot \nu(x) < 0 \end{aligned}$$

$$\begin{aligned}\psi_1(x,E,\Omega) &= u(x,E,\Omega) \text{ for } (x,E,\Omega)\in\partial V\times I\times S \\ &\quad \text{such that } \Omega\cdot\nu(x)<0,\end{aligned} \tag{23}$$

where I is an energy interval. The symbol u stands for the photon flux density on ∂V and $u\in L_2(\partial V\times I\times S)$. The boundary condition $\psi_1=u$ for $\Omega\cdot\nu(x)<0$ and $x\in\partial V$ means that the flux u is incoming outwardly on the patch ∂V and the boundary condition $\psi_j=0,(j=2,3)$ for $\Omega\cdot\nu(x)<0$ means that no other particles generate outward fluxes. The solution ψ is defined in the six-dimensional state space $G:=V\times I\times S$.

The variational form of the equation (22) with the stated boundary condition (23) is given in [35], and it is of the form

$$B(\psi,v)=F(v),\ v\in H^3, \tag{24}$$

where $B(\cdot,\cdot):H^3\times H^3\mapsto\mathbf{R}$ is the bilinear form, v is a test function, H is an appropriate Hilbert space,

$$\begin{aligned}B(\psi,v) &= -\langle\psi,\Omega\cdot\nabla v\rangle_{L_2(G)^3} \\ &+ \sum_{j=1}^{3}\int_S\int_I\int_{\partial V}(\Omega\cdot\nu)_+\psi_j v_j \mathrm{d}\sigma\mathrm{d}E\mathrm{d}\Omega+\langle K\psi,v\rangle_{L_2(G)^3}\end{aligned} \tag{25}$$

and

$$F(v)=\langle Q,v\rangle_{L_2(G)^3}+\int_S\int_I\int_{\partial V}(\Omega\cdot\nu)_- u v_1\mathrm{d}\sigma\mathrm{d}E\mathrm{d}\Omega, \tag{26}$$

where σ is the surface measure on ∂V. The subscript "$_+$" refers to the positive part of the function and the subscript "$_-$" refers to the negative part of the function.

Dose computation

We compute the dose in the following way. The incoming flux density of the l^{th} field S_l is u_l. It is assumed that $u_l\in L_2(\Gamma_l\times I\times S)$, where Γ_l is a patch of ∂V where the radiation is entering the domain V. Here $\psi^l=(\psi_1^l,\psi_2^l,\psi_3^l)$ is the flux density corresponding to the field S_l, that is, ψ^l is the solution of the equation

$$(\Omega\cdot\nabla+K)\psi^l=0 \tag{27}$$

with the boundary condition

$$\begin{aligned}\psi_2^l(x,E,\Omega) &= \psi_3^l(x,E,\Omega)=0 \text{ for } (x,E,\Omega)\in\partial V\times I\times S \\ &\quad \text{such that } \Omega\cdot\nu(x)<0 \\ \psi_1^l(x,E,\Omega) &= 0,\ \text{for } (x,E,\Omega)\in(\partial V\setminus\Gamma_l)\times I\times S \\ &\quad \text{such that } \Omega\cdot\nu(x)<0 \\ \psi_1^l(x,E,\Omega) &= u_l(x,E,\Omega) \text{ for } (x,E,\Omega)\in\Gamma_l\times I\times S \\ &\quad \text{such that } \Omega\cdot\nu(x)<0.\end{aligned} \tag{28}$$

We define $u \in L_2(\partial V \times I \times S)$ such that

$$u = \sum_{l=1}^{L} u_l \chi_l, \tag{29}$$

where $\chi_l : \partial V \times I \times S \to \mathbf{R}$ are the characteristic functions of $\Gamma_l \times I \times S$ $(l = 1, \ldots, L)$. Let $\psi = (\psi_1, \psi_2, \psi_3)$ be the solution of problem (22) with the boundary condition (23) where u is defined by (29). The solution of problem (22)-(23) is

$$\psi = (\sum_{l=1}^{L} \psi_1^l, \sum_{l=1}^{L} \psi_2^l, \sum_{l=1}^{L} \psi_3^l), \tag{30}$$

where ψ^l $(l = 1, ..., L)$ are the solutions of (27)-(28). Now the total dose distribution $D(x)$ from the incoming fields S_l $(l = 1, ..., L)$ at a point x of the patient domain V can be obtained from the measurement integral

$$D(x) = \sum_{j=2}^{3} \int_S \int_I \kappa_j(x, E) \psi_j(x, E, \Omega) \mathrm{d}E \mathrm{d}\Omega, \tag{31}$$

where $\kappa_j(x, E)$ are known stopping power factors for electrons and positrons and ψ is the solution of (24) with $u = \sum_{l=1}^{L} u_l \chi_l$.

Discrete finite element model for radiotherapy

For computer needs, the model presented has to be discretized, and we use the finite element method (FEM) because the inflow boundary condition is quite easy to handle via variational formulations.

To clarify the u-dependence of variables, we denote $\psi = \psi(u)$ if needed. Let $F : L_2(\partial V \times I \times S) \mapsto (H^3)^*$ (where * refers to the adjoint space, see [35] be the operator defined by

$$(Fu)(v) = \int_S \int_I \int_{\partial V} (\Omega \cdot \nu)_- u v_1 \mathrm{d}\sigma \mathrm{d}E \mathrm{d}\Omega. \tag{32}$$

Note that $F(v) = (Fu)(v)$. Using these notations $\psi = \psi(u)$ satisfies the variational equation

$$B(\psi(u), v) = (Fu)(v), \ v \in H^3. \tag{33}$$

Let X_h be a finite dimensional subspace of H^3 and let Y_h be a finite dimensional subspace of $L_2(\partial V \times I \times S)$. Denote a basis of X_h by $\{v_1, ..., v_N\}$ and denote a basis of Y_h by $\{w_1, ..., w_M\}$. Let

$$\psi_h = \sum_{n=1}^{N} \alpha_n v_n, \ u_h = \sum_{m=1}^{M} \beta_m w_m. \tag{34}$$

Now the FEM approximation of the variational equation (33) is defined as

$$B(\psi_h, v) = (Fu_h)(v),\ v \in X_h. \tag{35}$$

This leads to the system of equations

$$\mathbf{A}\alpha = \mathbf{B}\beta, \tag{36}$$

where $\mathbf{A} \in M(N \times N),\ \mathbf{B} \in M(N \times M)$ such that $\mathbf{A}(k,n) = B(v_n, v_k)$ and $\mathbf{B}(k,m) = (Fw_m)(v_k)$. In addition, we have vectors $\alpha = (\alpha_1, \ldots, \alpha_N)^T$ and $\beta = (\beta_1, \ldots, \beta_M)^T$. Equation (36) can be expressed in the form

$$(\,\mathbf{A} \quad -\mathbf{B}) \begin{pmatrix} \alpha \\ \beta \end{pmatrix} = 0, \tag{37}$$

which is actually the variational equation (33) in its discrete form.

Parameterization of the discrete finite element model

We say that the equation (37) is parameterized by a matrix $\mathbf{S} \in M(N+M, p)$ if

$$(\,\mathbf{A} \quad -\mathbf{B}) \begin{pmatrix} \alpha \\ \beta \end{pmatrix} = 0 \Leftrightarrow \begin{pmatrix} \alpha \\ \beta \end{pmatrix} = \mathbf{S}\gamma,\ \gamma \in \mathbf{R^P}. \tag{38}$$

Let $p_1,\ p_2$ be the canonical projections

$$p_1 : \mathbf{R^{N+M}} \to \mathbf{R^N} \tag{39}$$

$$p_2 : \mathbf{R^{N+M}} \to \mathbf{R^M}. \tag{40}$$

Denote $\mathbf{S}_j\gamma = p_j(\mathbf{S}\gamma)$ $(j = 1, 2)$. Then $\alpha = \mathbf{S}_1\gamma$ and $\beta = \mathbf{S}_2\gamma$. Hence we can denote

$$\psi \approx \psi_h = \sum_{n=1}^{N} \alpha_n v_n = \sum_{n=1}^{N} (\mathbf{S}_1\gamma)_n v_n := S_1\gamma \tag{41}$$

and

$$u \approx u_h = \sum_{m=1}^{M} \beta_m w_m = \sum_{m=1}^{M} (\mathbf{S}_2\gamma)_m w_m := S_2\gamma, \tag{42}$$

where $\gamma \in \mathbf{R^P}$. With finite elements, the matrices $\mathbf{A}$ and $\mathbf{B}$ have full rank and that is why we have here $p = M$.

After the parameterization, the dose can be approximately solved from the equation

$$D(x) \approx D\gamma(x) = \sum_{j=2}^{3} \int_S \int_I \kappa_j(x, E)(S_1\gamma)_j(x, E, \Omega)\mathrm{d}E\mathrm{d}\Omega. \tag{43}$$

In optimization, γ is the vector of decision variables.

Singular value decomposition (SVD) can be used in the parameterization of the discrete system, that is, in finding the matrix $\mathbf{S}$. Parameterization makes it possible to optimize large problems based on the finite element model. After parameterization, the number of unknown variables is decreased from $N + M$ to M. Parameterization of the system $(\,\mathbf{A} \quad -\mathbf{B}) \begin{pmatrix} \alpha \\ \beta \end{pmatrix} = 0$ is considered in more detail in [35].

Received: February, 2009